



Decreased expression of hsa_circ_0112879 in oral squamous cell carcinoma and its clinicopathological implications

Yufan Wang^{1#}, Shuai Sun^{2#}, Yuling Chen¹, Jianrong Li¹, Yuntao Lin¹, Li Wu¹, Huan Jing¹, Yuehong Shen¹, Hongyu Yang¹

¹Department of Oral and Maxillofacial Surgery, Peking University Shenzhen Hospital, Shenzhen, China; ²Department of Stomatology, Shenzhen Traditional Chinese Medicine Hospital, Shenzhen, China

Contributions: (I) Conception and design: Y Wang, S Sun, Y Shen, H Yang; (II) Administrative support: H Yang; (III) Provision of study materials or patients: Y Wang, H Yang; (IV) Collection and assembly of data: S Sun, Y Chen, Y Lin, L Wu; (V) Data analysis and interpretation: Y Wang, H Jing; (VI) Manuscript writing: All authors; (VII) Final approval of manuscript: All authors.

[#]These authors contributed equally to this work.

Correspondence to: Hongyu Yang, PhD. Department of Oral and Maxillofacial Surgery, Peking University Shenzhen Hospital, 1120 Lianhua Road, Futian District, Shenzhen 518001, China. Email: hyang192@hotmail.com.

Background: To identify differently expressed circular RNA (circRNA) in oral squamous cell carcinoma (OSCC) and adjacent normal tissue, construct a hsa_circ_0112879-related microRNAs (miRNAs) prognostic model, and discuss the circRNA as a biomarker for early diagnosis of OSCC.

Methods: The expression of hsa_circ_0112879 in OSCC cell lines and tissues was detected by quantitative real-time polymerase chain reaction (qRT-PCR). A receiver operating characteristic (ROC) curve was plotted to estimate its clinical significance. The potential miRNA and messenger RNA (mRNA) binding to hsa_circ_009755 were predicted by R software edgeR package. Based on the median value of the risk score in the all-sample cohort, all the included patients with OSCC were divided into either high- or low-risk groups, and Kaplan-Meier analysis was performed. The ROC curve was used to verify the accuracy of the risk signature in predicting the prognosis of OSCC. By univariable Cox, least absolute shrinkage and selection operator (LASSO), and multivariable Cox analyses, we constructed a hsa_circ_0112879-related miRNAs risk model to forecast the prognosis of OSCC.

Results: The expression of hsa_circ_0112879 was significantly downregulated in the OSCC tissues and cell lines. The expression level was statistically correlated with the pathological differentiation of OSCC tumors ($P=0.0285$). Furthermore, 141 differentially expressed hsa_circ_0112879-related miRNAs were obtained [$|\log_2FC| > 1$, false discovery rate (FDR) < 0.05], of which 70 miRNAs were up-regulated in OSCC tissues, whereas 71 miRNAs were down-regulated in OSCC tissues. The area under the ROC curve (AUC) at 1-, 3-, and 5-year in the all-sample cohort was 0.591, 0.689, and 0.618, respectively. The toll-like receptor signaling pathway, Janus tyrosine kinase-signal transducer and activator of transcription (JAK-STAT) signaling pathway, nucleotide-binding and oligomerization domain (NOD)-like receptor signaling pathway, and T-cell receptor (TCR) signaling pathway were mainly enriched in the high-risk group.

Conclusions: The model and nomogram constructed herein has the ability to discriminate the prognosis of OSCC patients. Hsa_circ_0112879 may serve as a novel biomarker in the diagnosis and prognosis of OSCC.

Keywords: Cancer; circular RNAs (circRNAs); biomarker

Submitted Feb 01, 2023. Accepted for publication Aug 01, 2023. Published online Sep 18, 2023.

doi: 10.21037/tcr-23-140

View this article at: <https://dx.doi.org/10.21037/tcr-23-140>

Introduction

There are close to 370,000 new oral cancer cases diagnosed every year, 2/3 of which are diagnosed in developing countries (1). Approximately over 90% of oral malignancies are of oral squamous cell carcinoma (OSCC) (2). The 5-year survival rate of OSCC patients remains below 65% (3), and the prognosis for patients that have advanced OSCC is often particularly poor (4). When tumors are detected at an early-stage, the 5-year overall survival (OS) can be notably improved to 85% or above (5). Under these circumstances, it is imperative to seek out novel biomarkers to support early tumor detection and treatments for OSCC.

Circular RNA (circRNA) is a newly identified class of non-coding RNA molecules with a closed loop structure (6). CircRNAs, initially reported to be the product of endogenous RNA splicing errors, are considered a non-functional product (7). Recently, numerous findings have revealed that the expression of circRNAs varies greatly across species (8,9). A growing number of studies have shown that circRNAs have multiple biological activities which are extensively involved in binding of RNA and proteins (10), acting as microRNA (miRNA) sponges (11), enabling RNA transport, and regulating translation (12). However, many functions of circRNAs in OSCC currently remain unknown.

This analysis identified hsa_circ_0112879 as distinctly downregulated in OSCC cell lines and tissues. Furthermore, it also suggested that the expression of hsa_circ_0112879 could be statistically associated with the clinicopathologic differentiation and diagnosis of patients with OSCC. Our team utilized univariable Cox, least absolute shrinkage and selection operator (LASSO), and multivariable Cox

analyses to construct a hsa_circ_0112879-related miRNAs risk signature which can forecast the prognosis of OSCC patients. The analysis indicated that hsa_circ_0112879 has the potential to be a biomarker for diagnosis and prediction of prognosis of OSCC. We present this article in accordance with the TRIPOD reporting checklist (available at <https://tcr.amegroups.com/article/view/10.21037/tcr-23-140/rc>).

Methods

Patients and tissue samples

Tissue samples were obtained from patients undergoing surgery in the Oral and Maxillofacial Surgery Department of Peking University Shenzhen Hospital. All tissues and their paired para-cancerous histologically normal tissues were collected and pathologically confirmed during surgery. After resection, the tissues were quickly transferred to -80°C for freezing and storage. The research protocol was approved by the Ethics Committee of Peking University Shenzhen Hospital (approval No. 2022-117). The study was conducted in accordance with the Declaration of Helsinki (as revised in 2013). All the included patients had given written informed consent.

Cell culture

The human OSCC cell lines SCC9, SCC15, SCC25, and CAL27 were purchased from the American Type Culture Collection (ATCC; Manassas, VA, USA). The human oral keratinocyte (HOK) cell line was acquired from the Chinese Academy of Sciences (Shanghai, China). The human oral squamous carcinoma SCC9 cell line was cultured in Dulbecco's modified Eagle medium (DMEM)/F12 medium with 10% fetal bovine serum (FBS; Gibco, Waltham, MA, USA). Other cells were cultured in DMEM (Gibco, Shanghai, China) also supplemented with FBS to a final concentration of 10%. The cells were grown in an incubator at 37°C with 5% CO_2 .

Quantitative real-time polymerase chain reaction (qRT-PCR)

RNA was extracted from tissue samples and cells using TRIzol reagent (Invitrogen, Carlsbad, CA, USA) according to manufacturer's instructions. The concentration and purity of the RNA was then determined using a

Highlight box

Key findings

- The expression of hsa_circ_0112879 could be statistically associated with the clinicopathologic differentiation and diagnosis of patients with oral squamous cell carcinoma (OSCC).

What is known and what is new?

- CircRNAs have multiple biological activities which are extensively involved in binding of RNA and proteins, acting as miRNA sponges, enabling RNA transport, and regulating translation.
- The functions of circRNAs in OSCC currently remain unknown.

What is the implication, and what should change now?

- Hsa_circ_0112879 has the potential to be a biomarker for diagnosis and prediction of prognosis of OSCC.

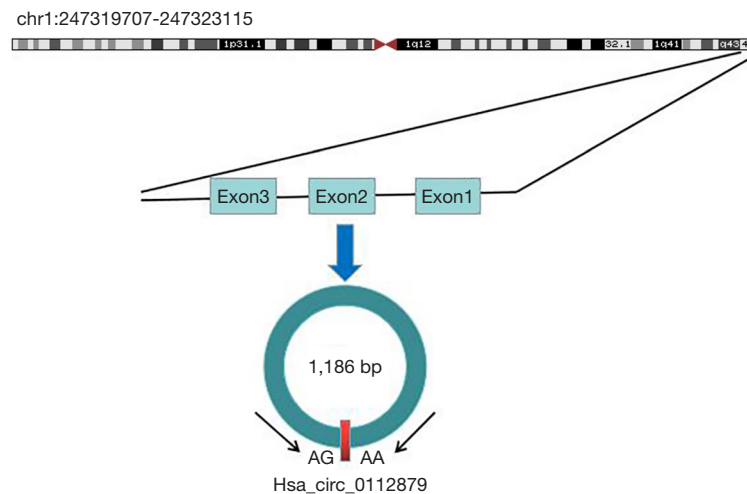


Figure 1 Hsa_circ_0112879 is encoded by the chromosomal region 1q44. Three exons form hsa_circ_0112879 from exon1 to exon3.

spectrophotometer (NanoDrop; Thermo Fisher Scientific, Waltham, MA, USA). Total RNA was reverse-transcribed into complementary DNA using PrimeScript RT Master Mix (Takara Bio, Shiga, Japan). The qRT-PCR was performed with SYBR-Green Premix Ex Taq (Takara Bio, Japan). Reaction was first performed at 95 °C for 5 seconds, 60 °C for 30 seconds, and 72 °C for 20 seconds, which was then repeated for a total of 40 cycles. The relative expression levels of hsa_circ_0112879 were measured using *ACTB* as an internal reference gene. The sequences of the hsa_circ_0112879 primers were as follows: forward primer 5'-GAGAGAACTGTGAATGTAAGGTGT-3' and reverse primer 5'-CAACAAAGCCCCTCCTCCT-3'. The primer sequences used for *ACTB* forward primer were 5'-AACTGGAACGTTGAGAGTG-3' and reverse primer were 5'-AGTGGTCTGGCTTTTAGGT-3'. The ΔC_t or the $2^{-\Delta\Delta C_t}$ method were used for comparative quantification (13). The test for each sample was repeated more than 3 times independently.

Construction and analysis of Hsa_circ_0112879-related miRNA prognostic model

Transcriptome data and clinical data used in this study come from The Cancer Genome Atlas database (TCGA; <https://portal.gdc.cancer.gov/repository>). Our team utilized univariable Cox, LASSO, and multivariable Cox analyses to construct a hsa_circ_0112879-related miRNAs risk signature that can predict the prognosis of OSCC patients.

Statistical analysis

GraphPad Prism software (version 5.0; GraphPad Software, San Diego, CA, USA) was used for statistical analysis and drawing. Paired *t*-test was used to correlate the expression levels of hsa_circ_0112879 between OSCC cell lines and normal cells or between patient samples and adjacent normal samples. The correlation between the expression of hsa_circ_0112879 and the clinicopathological factors were analyzed using unpaired *t*-test and Bartlett's test for equal variances. Also, the diagnostic values were obtained from the receiver operating characteristic (ROC) curve. Statistical significance was considered when $P < 0.05$.

Results

Expression of hsa_circ_0112879 in OSCC tissues

Hsa_circ_0112879, one of the circRNAs primarily identified in the mammalian brain, has a splice length of 1,168 base pairs (bp) (14) and is located within the *ZNF124* gene at the chromosomal position chr1:247319707-247323115 (Figure 1). Based on our qRT-PCR and ROC analysis, we observed that the expression of hsa_circ_0112879 was markedly down-regulated in OSCC samples as compared to expression of their adjacent normal tissues ($P < 0.001$) (Figure 2).

Expression levels of hsa_circ_0112879 in OSCC cell lines

Next, we analyzed the expression levels of hsa_circ_0112879

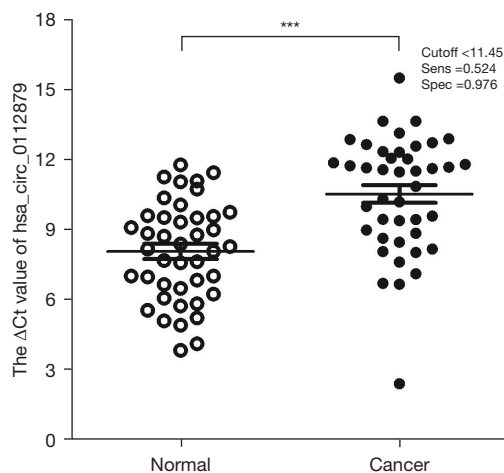


Figure 2 Expression of hsa_circ_0112879 in OSCC tissues and adjacent normal tissues. The expression of hsa_circ_0112879 is significantly down-regulated in OSCC tissues as compared to adjacent normal tissues (n=42, ***, $P < 0.001$). Higher value indicates lower expression. The cutoff for expression of hsa_circ_0112879 was 11.45 and the sensitivity and specificity values were 0.524 and 0.976, respectively. Data are represented as mean \pm SD of three independent experiments. OSCC, oral squamous cell carcinoma; SD, standard deviation.

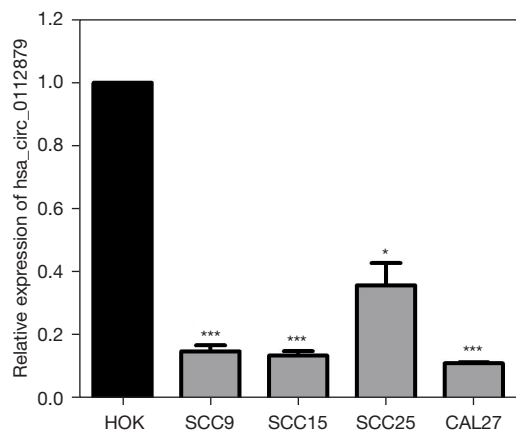


Figure 3 Expression of hsa_circ_0112879 in OSCC cell lines. Expression levels of hsa_circ_0112879 in four OSCC cell lines (SCC9, SCC15, SCC25, and CAL27) and HOK cells were determined by qRT-PCR. Data are expressed as mean \pm SD of three independent experiments. *, $P < 0.05$; ***, $P < 0.001$. HOK, human oral keratinocyte; OSCC, oral squamous cell carcinoma; qRT-PCR, quantitative real-time polymerase chain reaction; SD, standard deviation.

in the oral normal cell HOK and different OSCC cell lines—SCC9, SCC15, SCC25, and CAL27. We found that in the OSCC cell lines, the expression of hsa_circ_0112879 was obviously reduced compared to HOK cells (Figure 3).

Clinicopathological characteristics of OSCC patients

The 42 OSCC patients (12 women and 30 men) were aged 29–78 years (median 54 years). These 42 cases included 13 well-differentiated tumors (31%), 23 moderately-differentiated tumors (54.8%), and 6 poorly-differentiated cases (14.2%). The tumor staging analysis suggested that 4 cases were in the T1–T2 stage (57.1%), whereas 18 cases were in the T3–T4 stage (42.9%). Moreover, patients were diagnosed with differential lymph-node involvement: 25 cases presented with lymph-node negative (N0) tumors (60%), whereas 17 cases presented lymph-node positive (N1–N3) tumors (40%). The other clinicopathological information about the patients has been summarized and organized in Table 1.

The role of hsa_circ_0112879 in the diagnosis of OSCC

We investigated the correlation between hsa_circ_0112879 expression level and clinicopathological data (Table 2). The analysis suggested that the expression level of hsa_circ_0112879 was statistically associated with pathological differentiation of OSCC tumors ($P = 0.0285$). However, we could not observe correlation between the expression levels of hsa_circ_0112879 and age, gender, tumor size, T stage, tumor-node-metastasis (TNM) stage, and lymph node metastasis. Also, the area under the ROC curve (AUC) analysis used to distinguish OSCC tissues from their paired adjacent normal tissues provided a value of 0.798 [95% confidence interval (CI): 0.705–0.891; $P < 0.001$; Figure 4]. The cutoff of hsa_circ_0112879 expression was 11.45, with a sensitivity of 0.524 and a specificity value of 0.976 (Figure 2).

Predicting and screening of circRNA related miRNA

A total of 1,126 miRNAs targeting hsa_circ_0112879 were predicted by using the online database. The 1,126 hsa_circ_0112879-related miRNAs in 247 OSCC samples and 17 normal samples were analyzed by R software edgeR package (R Foundation for Statistical Computing, Vienna,

Table 1 Primer sequences

Primer set	Forward primer	Reverse primer
hsa_circ_0112879	GAGAGAACTGTGAATGTAAGGTGT	CAACAAAGCCCACTCCTCCT
β-Actin	AAACTGGAACGTTGAGAGTG	AGTGGTCTGGCTTTTAGGT

Table 2 Relationship of hsa_circ_0112879 expression levels (ΔCt) in OSCC tissues with clinicopathological factors of OSCC patients

Characteristics	No. of patients (%)	P value
Gender		0.929
Male	30 (71.4)	
Female	12 (28.6)	
Age (years)		0.152
≥60	15 (35.7)	
<60	27 (64.3)	
Tumor size (cm)		0.298
≥5	7 (16.7)	
<5	35 (83.3)	
Differentiation grade		0.0285*
Well	13 (31.0)	
Moderately	23 (54.8)	
Poorly	6 (14.2)	
T stage		0.486
T1–2	24 (57.1)	
T3–4	18 (42.9)	
TNM		0.317
I & II	17 (40.0)	
III & IV	25 (60.0)	
Lymphatic metastasis		0.642
N0	25 (60.0)	
N1–3	17 (40.0)	

*, significant association. OSCC, oral squamous cell carcinoma; TNM, tumor-node-metastasis.

Austria). From the results, 141 differentially expressed hsa_circ_0112879-related miRNAs were obtained [$|\log_2FC| > 1$, false discovery rate (FDR) < 0.05], of which 70 miRNAs were up-regulated in OSCC tissues, whereas 71 miRNAs were down-regulated in OSCC tissues (Figure 5). Altogether, 34 hsa_circ_0112879-related miRNAs with prognostic values were obtained (Figure 6A). Then, in

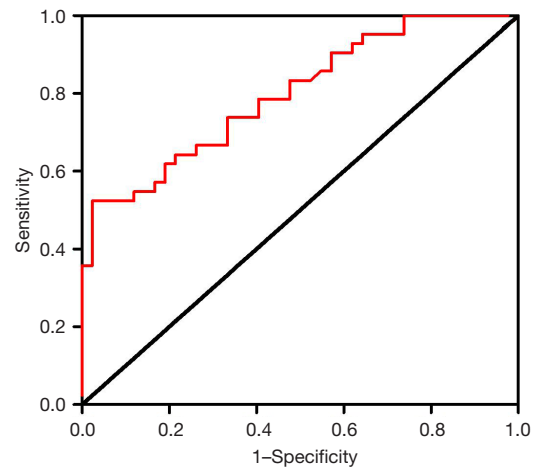


Figure 4 The diagnostic value of hsa_circ_0112879 in OSCC. AUC was 0.798 (95% CI: 0.705–0.891, $P < 0.001$). OSCC, oral squamous cell carcinoma; AUC, area under the ROC curve; CI, confidence interval; ROC, receiver operating characteristic.

order to optimize our model, we used LASSO regression analysis and cross-validation to further filter, and 21 most representative candidate miRNAs were found (Figure 6B). Among these 21 candidate miRNAs, we selected 3 miRNAs of interest: hsa-miR-654-3p, hsa-miR-338-3p, and hsa-miR-155-3p, and clarified their binding sites to hsa_circ_0112879 (Figure 6B). Multivariable Cox regression analyses were performed on these 3 candidate miRNAs, and their corresponding coefficients were finally obtained and then utilized to construct the prognostic model (Table 3).

Construction of a hsa_circ_0112879-related miRNA prognostic model

Formula: Risk score = $\sum_4^i a_i * b_i$ (a: coefficients, b: gene expression level). According to the median value of the risk score in the all-sample cohort described above, all patients with OSCC were grouped as either high- or low-risk and were subjected to Kaplan-Meier analysis. In the results, OS was significantly lower in the high-risk group than in the low-risk group (Figure 6C). The ROC curve

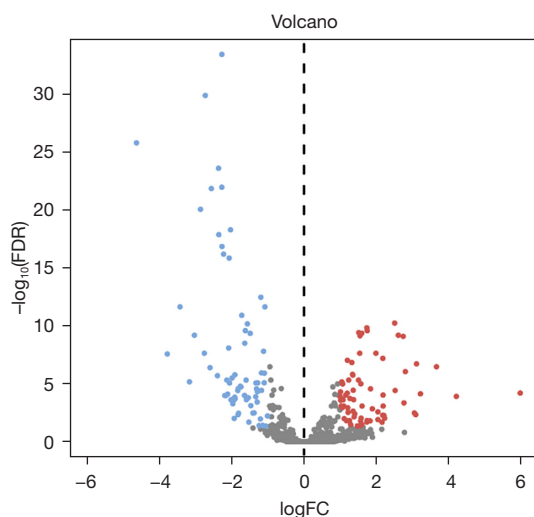


Figure 5 The volcano plot of differentially expressed hsa_circ_0112879-related miRNAs between OSCC tissue and normal tissue. 141 differentially expressed hsa_circ_0112879-related miRNAs were obtained ($|\log_2FC| > 1$, $FDR < 0.05$), of which 70 miRNAs were up-regulated in OSCC tissues, while 71 miRNAs were down-regulated in OSCC tissues (blue: down-regulated miRNAs; red: up-regulated miRNAs). FDR, false discovery rate; FC, fold change; OSCC, oral squamous cell carcinoma; miRNAs, microRNAs.

was used to verify the accuracy of the risk signature in forecasting the prognosis of OSCC (Figure 6D). The AUC of 1-, 3-, and 5-year survival in the all-sample cohort was 0.591, 0.689, and 0.618, respectively. We also evaluated the relationship between risk score and OSCC patients by univariate and multivariate Cox regression analysis, and the results showed that risk score could be an independent factor affecting the prognosis of OSCC patients (Figure 6E). Moreover, we established a nomogram based on 4 clinical factors (age, gender, grade, stage) and risk scoring for the quantitative prediction of 1-, 3-, and 5-year survival in OSCC patients (Figure 7A). Both risk score and stage may be the independent prognostic indicators for OSCC patients. Subsequently, the prediction ability and accuracy of nomograph model were verified by calibration curve (Figure 7B). By performing gene set enrichment analysis (GSEA), filtered by q -value < 0.05 , the result showed that Toll-like receptor signaling pathway, Janus tyrosine kinase-signal transducer and activator of transcription (JAK-STAT) signaling pathway, nucleotide-binding and oligomerization domain (NOD)-like receptor signaling pathway, and T-cell receptor (TCR) signaling pathway were mainly enriched

in the high-risk group (Figure 8). However, the low-risk group's pathways with $P < 0.05$ were not enriched.

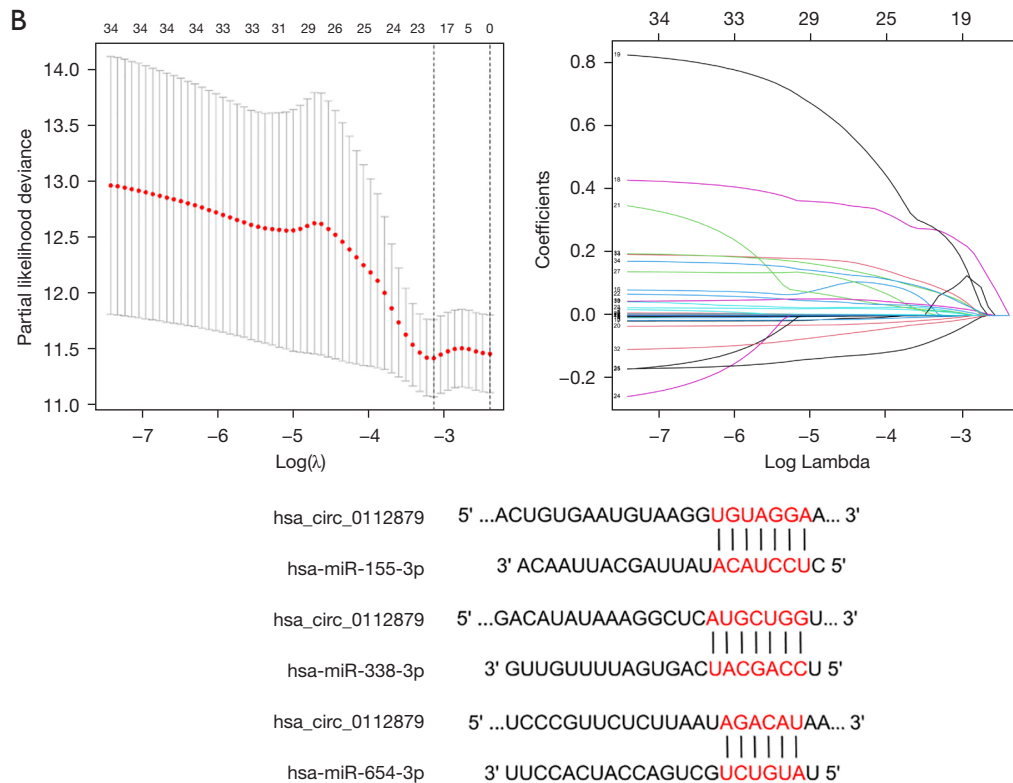
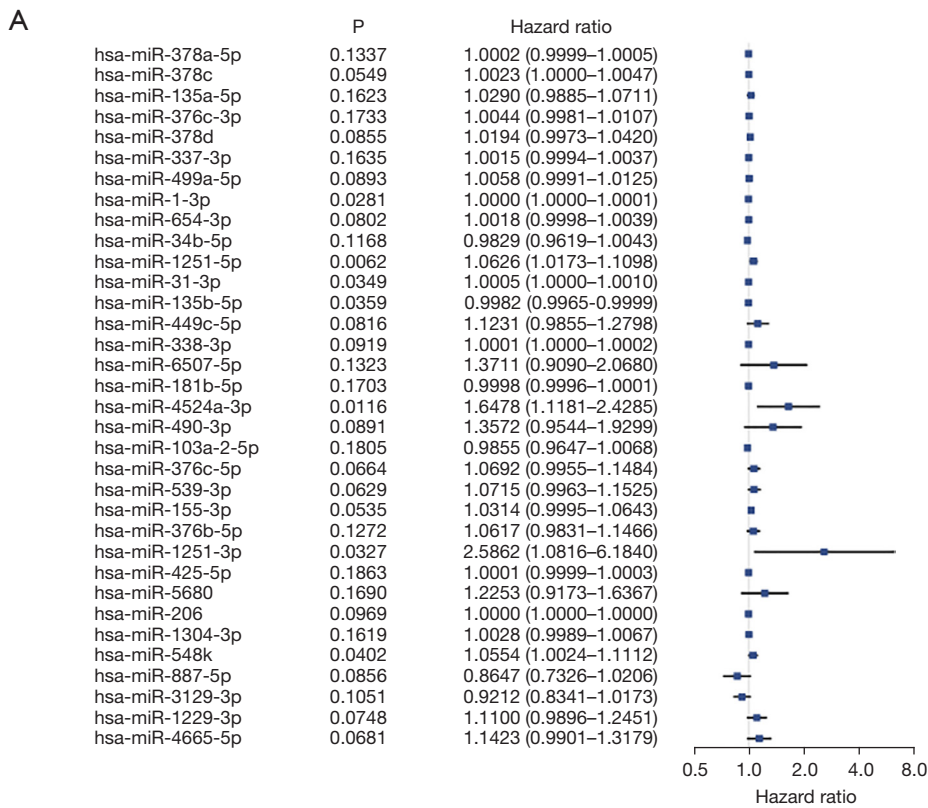
Discussion

OSCC is a commonly occurring malignancy of the head and neck (15). In recent decades, there has been considerable progress in the diagnosis and treatment of OSCC, but the mortality rate is maintained at a high level, generally due to its high recurrence rate and strong propensity to metastasize (16). Patients with OSCC are usually treated with surgical resection, radiotherapy, chemotherapy, and targeted therapy aiming to improve their quality of life, but still face difficulty in surviving (17). It is thus extremely important to discover molecular biomarkers that have a role to play for the treatment of OSCC.

CircRNAs are a novel form of endogenous non-coding RNA molecule formed by back-splicing with either exon or intron circularization, unlike other forms (18,19). Moreover, circRNAs are characterized by highly stable and highly conserved sequences (20). Also, the circRNAs exhibit tissue specificity, making them potential biomarkers for diagnosis of cancers (21).

There is growing evidence that circRNA is involved in many types of cancers, for example papillary thyroid carcinoma (22), glioma (23), breast cancer (24), and non-small cell lung cancer (25). Fan *et al.* found that circSPATA6 inhibited cell migration and invasion and could act as a sponge for miR-182, increasing TRAF6 expression and thus promoting OSCC progression (26). Meanwhile, hsa_circRNA_0009128 has been found to be upregulated in both OSCC tissues and cell lines, with its high expression associated with TNM stage and lymph node metastasis (27). Hsa_circRNA_100533 has been shown to regulate G-protein α_s (GNAS) affecting cell proliferation, migration, and cell apoptosis in OSCC by sponging the activity of hsa_miR_933 (28). Moreover, Li *et al.* identified that compared with the adjacent healthy tissues and normal cells, hsa_circ_0086414 is downregulated (29).

Here, we first identified hsa_circ_0112879 to be downregulated in OSCC tissues and cell lines. Additionally, we were able to statistically correlate the expression levels of hsa_circ_0112879 with pathological differentiation of OSCC tumors. Moreover, hsa_circ_0112879 might possess tumor-suppressive effects in OSCC, which needs to be confirmed via *in vitro* and *in vivo* studies using larger sample sets. Taken together, our findings emphasize the potential and valuable of hsa_circ_0112879 in the prognosis of OSCC.



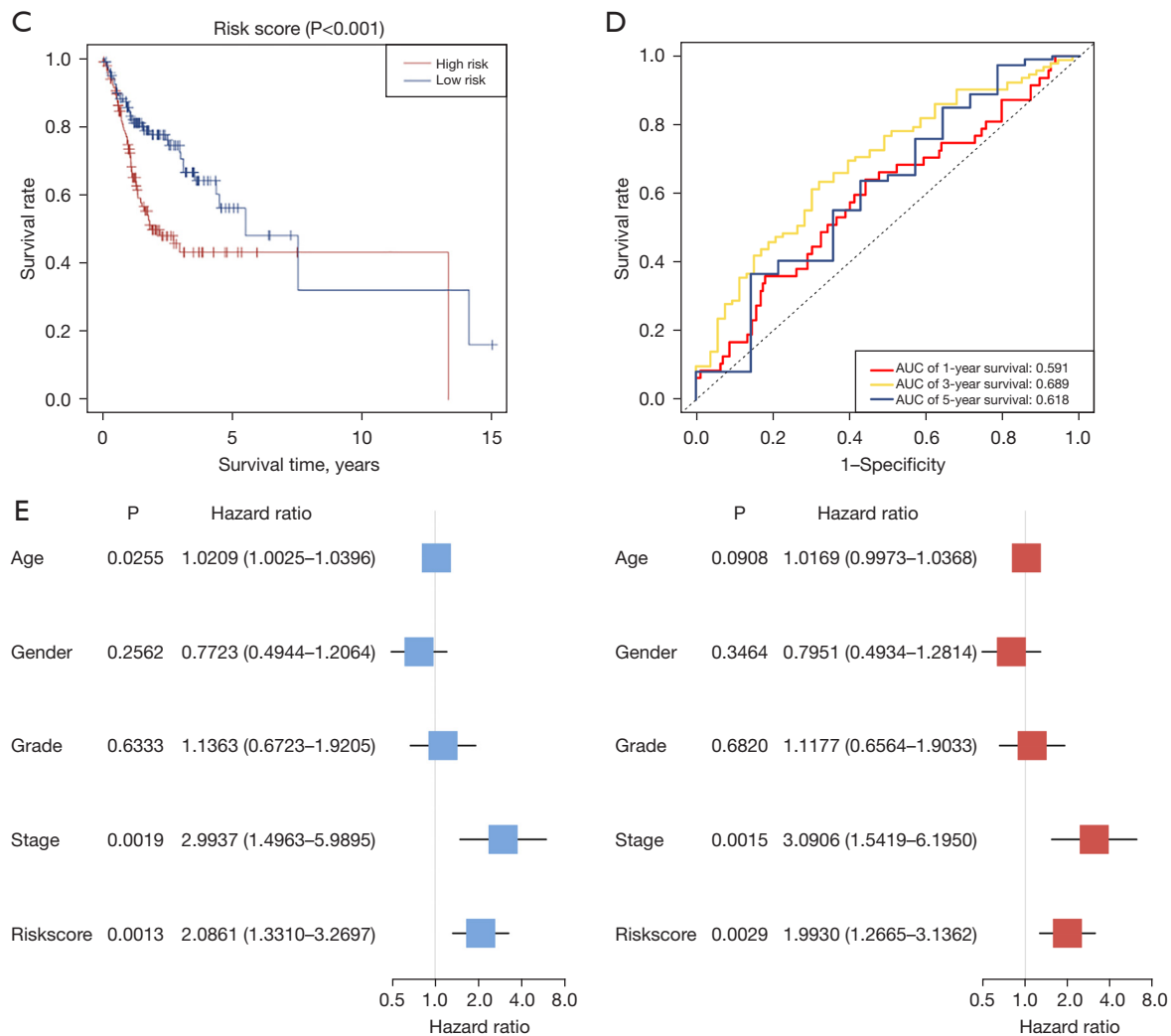


Figure 6 Construction of a hsa_circ_0112879-related miRNA prognostic model. (A) In the all-sample cohort, 141 differentially expressed hsa_circ_0112879-related miRNAs were analyzed by univariate Cox regression, and altogether 34 hsa_circ_0112879-related miRNAs with prognostic values were obtained. (B) 21 most representative candidate miRNAs were found and we selected three miRNAs of interest: hsa-miR-654-3p, hsa-miR-338-3p and hsa-miR-155-3p, and clarified their binding sites to hsa_circ_0112879. (C) OS was significantly lower in the high-risk group than in the low-risk group. (D) ROC curve was used to verify the accurateness of the risk signature in forecasting the prognoses of patients with OSCC. (E) The relationship between risk score and OSCC patients by univariate and multivariate Cox regression analysis, and the results showed that risk score could be an independent factor affecting the prognosis of OSCC patients. AUC, area under the ROC curve; ROC, receiver operating characteristic; miRNAs, microRNAs; OS, overall survival; ROC, receiver operating characteristic; OSCC, oral squamous cell carcinoma.

Table 3 Three candidate miRNAs by multivariate Cox regression analysis

Candidate miRNAs	Coefficient	HR	HR.95L	HR.95H	P value
hsa-miR-654-3p	0.0024	1.0025	1.0005	1.0046	0.0166
hsa-miR-338-3p	0.0001	1.0001	1.0000	1.0003	0.0675
hsa-miR-155-3p	0.0376	1.0393	1.0077	1.0719	0.0143

miRNA, microRNA; HR, hazard ratio; L, low; H, high.

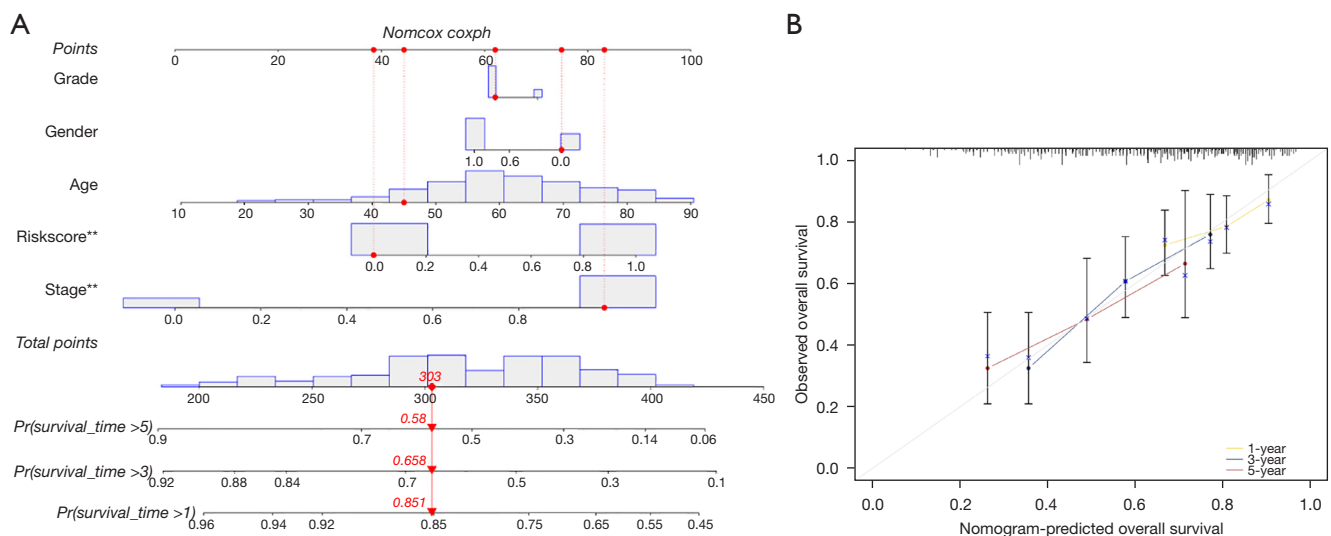


Figure 7 Construction of a nomogram based on risk scores. (A) A nomogram was established on the foundation of 4 clinical factors (age, gender, grade, stage) and risk scoring for the quantitative prediction of 1-, 3-, and 5-year survival in OSCC patients. Both risk score and stage can be used as independent prognostic indicators for OSCC patients. **, $P < 0.01$. (B) The calibration curve was employed to verify the predictive ability and accurateness of the nomograph model. OSCC, oral squamous cell carcinoma.

CircRNAs possess miRNA binding sites and have been reported to regulate gene expression through sponging. There are mounting studies reporting this type of regulation. Our current study also made predictions on whether hsa_circ_0112879 could affect the miRNAs in OSCC. Based on bioinformatics analysis, we found that hsa_circ_0112879 may have strong interactions with hsa-miR-654-3p, hsa-miR-338-3p, and hsa-miR-155-3p. Hsa-miR-654-3p, hsa-miR-338-3p, and hsa-miR-155-3p have been shown to play an important role in cancer. Hsa-miR-654-3p has been validated as an antitumor gene targeting *CREB1* to hamper malignant progression of sinonasal squamous cell carcinoma through miR-654-3p/*CREB1*/*PSEN1* axis (30). Hsa-miR-338-3p, which has been shown to be downregulated in glioblastoma, may affect the biogenesis and rapid proliferation of glioma cells (31). Hsa-miR-155-3p, as a proto-oncogene which is upregulated in OSCC, is responsible for intricate regulation of the progression of oral submucous fibrosis (OSMF) to OSCC via deregulated expression of c-Fos (32). In our study, multivariable Cox regression analyses were completed on those 3 candidate miRNAs, and finally, their corresponding coefficients were obtained, which were utilized to construct the prognostic model. The results show that the model has the ability to discriminate the prognosis of OSCC patients and risk score could be an independent factor affecting the prognosis of

OSCC patients. The nomogram constructed based on risk scores also has the ability to accurately estimate the OS of OSCC patients. Interestingly, GSEA revealed that Toll-like receptor signaling pathway, JAK-STAT signaling pathway, NOD-like receptor signaling pathway, and TCR signaling pathway were mainly enriched in the high-risk group. These all indicate that the model and nomogram based on hsa_circ_0112879 has the ability to accurately estimate the OS of OSCC patients. Of course, a further step for hsa_circ_0112879 research is to examine the interaction between hsa_circ_0112879 and miRNAs in OSCC and to clarify the downstream molecular mechanism of hsa_circ_0112879 in OSCC and whether it is similarly expressed in other cancers.

Conclusions

Our research shows that hsa_circ_0112879 is significantly downregulated in OSCC as compared to adjacent normal tissue, and that it associates with clinicopathological implications of this tumor type. The hsa_circ_0112879-related miRNA prognostic model shows the important role of hsa_circ_0112879 in OSCC. A thorough investigation of its mechanism of action and genomic interactions during progression of the disease should aid in use as a diagnostic and prognostic tumor marker.

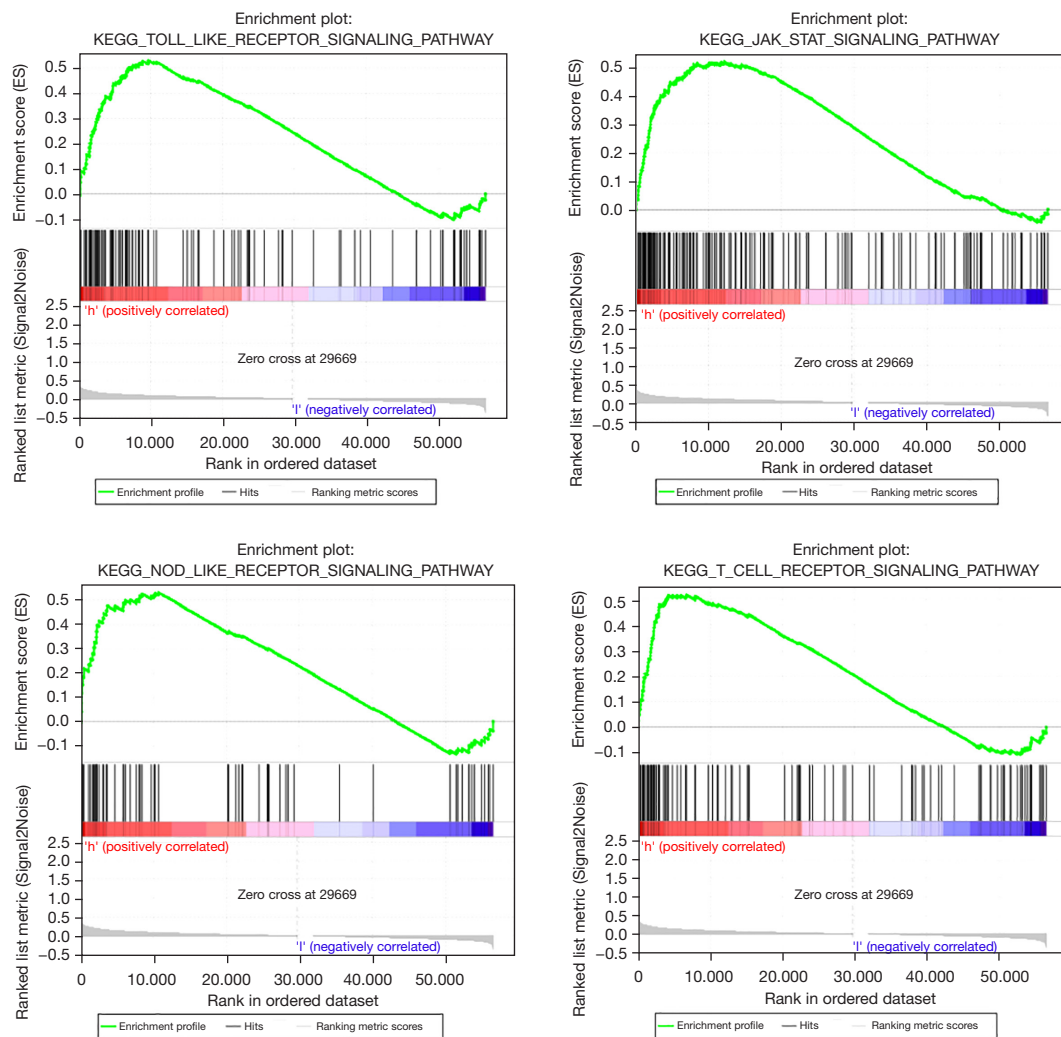


Figure 8 Gene set enrichment analysis results. Filtered by q -value < 0.05 , Toll-like receptor signaling pathway, JAK-STAT signaling pathway, NOD-like receptor signaling pathway, and TCR signaling pathway were mainly enriched in the high-risk group. JAK-STAT, Janus tyrosine kinase-signal transducer and activator of transcription; NOD, nucleotide-binding and oligomerization domain; TCR, T-cell receptor.

Acknowledgments

Funding: This study was supported by the Natural Science Foundation of Guangdong Province (Grant No. 2019A1515011911), the Research Program of Shenzhen Innovation Council of China (Grant Nos. JCYJ20200109140208058 and JCYJ20180228175511141), the National Natural Science Foundation of China (Grant No. 82000841), and Shenzhen Fund for Guangdong Provincial High-level Clinical Key Specialties (No. SZGSP008). This study was also supported by the Sanming Project of Medicine in Shenzhen (SZSM202111012, Oral and Maxillofacial Surgery Team, Professor Yu Guangyan,

Peking University Hospital of Stomatology).

Footnote

Reporting Checklist: The authors have completed the TRIPOD reporting checklist. Available at <https://tcr.amegroups.com/article/view/10.21037/tcr-23-140/rc>

Data Sharing Statement: Available at <https://tcr.amegroups.com/article/view/10.21037/tcr-23-140/dss>

Peer Review File: Available at <https://tcr.amegroups.com/>

[article/view/10.21037/tcr-23-140/prf](https://doi.org/10.21037/tcr-23-140/prf)

Conflicts of Interest: All authors have completed the ICMJE uniform disclosure form (available at <https://tcr.amegroups.com/article/view/10.21037/tcr-23-140/coif>). The authors have no conflicts of interest to declare.

Ethical Statement: The authors are accountable for all aspects of the work in ensuring that questions related to the accuracy or integrity of any part of the work are appropriately investigated and resolved. The research protocol was approved by the Ethics Committee of Peking University Shenzhen Hospital (approval No. 2022-117). The study was conducted in accordance with the Declaration of Helsinki (as revised in 2013). All the included patients had given written informed consent.

Open Access Statement: This is an Open Access article distributed in accordance with the Creative Commons Attribution-NonCommercial-NoDerivs 4.0 International License (CC BY-NC-ND 4.0), which permits the non-commercial replication and distribution of the article with the strict proviso that no changes or edits are made and the original work is properly cited (including links to both the formal publication through the relevant DOI and the license). See: <https://creativecommons.org/licenses/by-nc-nd/4.0/>.

References

- Ghantous Y, Abu Elnaaj I. Global incidence and risk factors of oral cancer. *Harefuah* 2017;156:645-9.
- Lingen MW, Kalmar JR, Karrison T, et al. Critical evaluation of diagnostic aids for the detection of oral cancer. *Oral Oncol* 2008;44:10-22.
- Chi AC, Day TA, Neville BW. Oral cavity and oropharyngeal squamous cell carcinoma--an update. *CA Cancer J Clin* 2015;65:401-21.
- Singhvi HR, Malik A, Chaturvedi P. The Role of Chronic Mucosal Trauma in Oral Cancer: A Review of Literature. *Indian J Med Paediatr Oncol* 2017;38:44-50.
- Takahashi H, Yanamoto S, Yamada S, et al. Effects of postoperative chemotherapy and radiotherapy on patients with squamous cell carcinoma of the oral cavity and multiple regional lymph node metastases. *Int J Oral Maxillofac Surg* 2014;43:680-5.
- Qu S, Liu Z, Yang X, et al. The emerging functions and roles of circular RNAs in cancer. *Cancer Lett* 2018;414:301-9.
- Hsu MT, Coca-Prados M. Electron microscopic evidence for the circular form of RNA in the cytoplasm of eukaryotic cells. *Nature* 1979;280:339-40.
- Memczak S, Jens M, Elefsinioti A, et al. Circular RNAs are a large class of animal RNAs with regulatory potency. *Nature* 2013;495:333-8.
- Nicolet BP, Engels S, Aglialoro F, et al. Circular RNA expression in human hematopoietic cells is widespread and cell-type specific. *Nucleic Acids Res* 2018;46:8168-80.
- Li Z, Huang C, Bao C, et al. Exon-intron circular RNAs regulate transcription in the nucleus. *Nat Struct Mol Biol* 2015;22:256-64.
- Hansen TB, Jensen TI, Clausen BH, et al. Natural RNA circles function as efficient microRNA sponges. *Nature* 2013;495:384-8.
- Zhang Z, Yang T, Xiao J. Circular RNAs: Promising Biomarkers for Human Diseases. *EBioMedicine* 2018;34:267-74.
- Livak KJ, Schmittgen TD. Analysis of relative gene expression data using real-time quantitative PCR and the 2(-Delta Delta C(T)) Method. *Methods* 2001;25:402-8.
- Rybak-Wolf A, Stottmeister C, Glažar P, et al. Circular RNAs in the Mammalian Brain Are Highly Abundant, Conserved, and Dynamically Expressed. *Mol Cell* 2015;58:870-85.
- Boscolo-Rizzo P, Da Mosto MC, Rampazzo E, et al. Telomeres and telomerase in head and neck squamous cell carcinoma: from pathogenesis to clinical implications. *Cancer Metastasis Rev* 2016;35:457-74.
- Galeone C, Edefonti V, Parpinel M, et al. Folate intake and the risk of oral cavity and pharyngeal cancer: a pooled analysis within the International Head and Neck Cancer Epidemiology Consortium. *Int J Cancer* 2015;136:904-14.
- Ren S, Cheng X, Chen M, et al. Hypotoxic and Rapidly Metabolic PEG-PCL-C3-ICG Nanoparticles for Fluorescence-Guided Photothermal/Photodynamic Therapy against OSCC. *ACS Appl Mater Interfaces* 2017;9:31509-18.
- Yang F, Zhu P, Guo J, et al. Circular RNAs in thoracic diseases. *J Thorac Dis* 2017;9:5382-9.
- Petkovic S, Müller S. RNA circularization strategies in vivo and in vitro. *Nucleic Acids Res* 2015;43:2454-65.
- Jeck WR, Sorrentino JA, Wang K, et al. Circular RNAs are abundant, conserved, and associated with ALU repeats. *RNA* 2013;19:141-57.
- Xia S, Feng J, Lei L, et al. Comprehensive characterization of tissue-specific circular RNAs in the human and mouse

- genomes. *Brief Bioinform* 2017;18:984-92.
22. Lou W, Ding B, Wang J, et al. The Involvement of the hsa_circ_0088494-miR-876-3p-CTNNB1/CCND1 Axis in Carcinogenesis and Progression of Papillary Thyroid Carcinoma. *Front Cell Dev Biol* 2020;8:605940.
 23. Song X, Zhang N, Han P, et al. Circular RNA profile in gliomas revealed by identification tool UROBORUS. *Nucleic Acids Res* 2016;44:e87.
 24. Liu Z, Zhou Y, Liang G, et al. Circular RNA hsa_circ_001783 regulates breast cancer progression via sponging miR-200c-3p. *Cell Death Dis* 2019;10:55.
 25. Li C, Zhang J, Yang X, et al. hsa_circ_0003222 accelerates stemness and progression of non-small cell lung cancer by sponging miR-527. *Cell Death Dis* 2021;12:807.
 26. Fan X, Wang Y. Circular RNA circSPATA6 Inhibits the Progression of Oral Squamous Cell Carcinoma Cells by Regulating TRAF6 via miR-182. *Cancer Manag Res* 2021;13:1817-29.
 27. Zhang H, Wang Z, Zhang Z. Hsa_circ_0009128 mediates progression of oral squamous cell carcinoma by influencing MMP9. *Oral Dis* 2023;29:661-71.
 28. Zhu X, Shao P, Tang Y, et al. hsa_circRNA_100533 regulates GNAS by sponging hsa_miR_933 to prevent oral squamous cell carcinoma. *J Cell Biochem* 2019;120:19159-71.
 29. Li L, Zhang ZT. Hsa_circ_0086414 Might Be a Diagnostic Biomarker of Oral Squamous Cell Carcinoma. *Med Sci Monit* 2020;26:e919383.
 30. Cui X, Yang Y, Yan A. MiR-654-3p Constrains Proliferation, Invasion, and Migration of Sinonasal Squamous Cell Carcinoma via CREB1/PSEN1 Regulatory Axis. *Front Genet* 2022;12:799933.
 31. Wang WY, Lu WC. Reduced Expression of hsa-miR-338-3p Contributes to the Development of Glioma Cells by Targeting Mitochondrial 3-Oxoacyl-ACP Synthase (OXSM) in Glioblastoma (GBM). *Onco Targets Ther* 2020;13:9513-23.
 32. Chugh A, Purohit P, Vishnoi JR, et al. Correlation of hsa miR-101-5p and hsa miR-155-3p Expression With c-Fos in Patients of Oral Submucous Fibrosis (OSMF) and Oral Squamous Cell Carcinoma (OSCC). *J Maxillofac Oral Surg* 2023;22:381-7.

Cite this article as: Wang Y, Sun S, Chen Y, Li J, Lin Y, Wu L, Jing H, Shen Y, Yang H. Decreased expression of hsa_circ_0112879 in oral squamous cell carcinoma and its clinicopathological implications. *Transl Cancer Res* 2023;12(10):2875-2886. doi: 10.21037/tcr-23-140